# The Bainite Transformation: Unresolved Issues

H. K. D. H. Bhadeshia

University of Cambridge
Department of Materials Science and Metallurgy
Pembroke Street, Cambridge CB2 3QZ, U.K.
hkdb@cus.cam.ac.uk www.msm.cam.ac.uk/phase–trans

## ABSTRACT

A great deal of research, over many decades since the discovery of bainite, has revealed substantial information about the mechanism of the bainite transformation in steels. Elements of the theory are now routinely being used in many parts of the world in the design of novel alloys and in the interpretation of a variety of experimental data. However, there remain some difficulties which are holding up technological progress. Two of these, the precipitation of carbides and the formation of bainite from plastically deformed austenite, are reviewed in the hope that further progress can be stimulated, particularly with respect to the development of quantitative models.

## INTRODUCTION

Science is essentially empirical; for example, there is no fundamental justification for the conservation of energy other than the fact that the principle has thus far stood the test of time. A further difficulty is that there are always loose ends in all known theories. Consequently, the assessment of unresolved issues requires a definition of what is meant by "resolved", particularly when considering the bainite transformation which has been the subject of much discussion. A good scheme would be to follow Hawkins [1], who makes the reasonable proposition that a theory must satisfy at least two criteria. Firstly, it must describe a large class of observations with few arbitrary parameters. And secondly, it must make predictions which can be verified or disproved.

A simple theory, the elements of which were first proposed by Hehemann and coworkers [2], elegantly fits these criteria. It has subsequently been developed and has survived the panoply of experimental techniques available today. The details of the theory have been reviewed extensively [3–5] so it is not the intention here to repeat the story. Nevertheless, a brief introduction is presented in order to set the scene for the discussion of unresolved topics where research could be focussed.

## OVERVIEW OF TRANSFORMATION MECHANISM

Bainite nucleates like martensite but with the partitioning of interstitial carbon [6]. The surface to volume ratio decreases beyond the nucleation stage, making it possible for growth to occur without any diffusion. The growth process is illustrated in Fig. 1, [7]. A plate or lath of bainite grows by a martensitic mechanism but because the transformation occurs at a relatively high temperature, the excess carbon soon afterwards partitions into the residual austenite. The carbon then precipitates from the austenite giving the inter–plate carbides typical of an upper bainitic microstructure. This post–transformation diffusion process slows down as the transformation temperature is reduced, thereby providing an opportunity for some

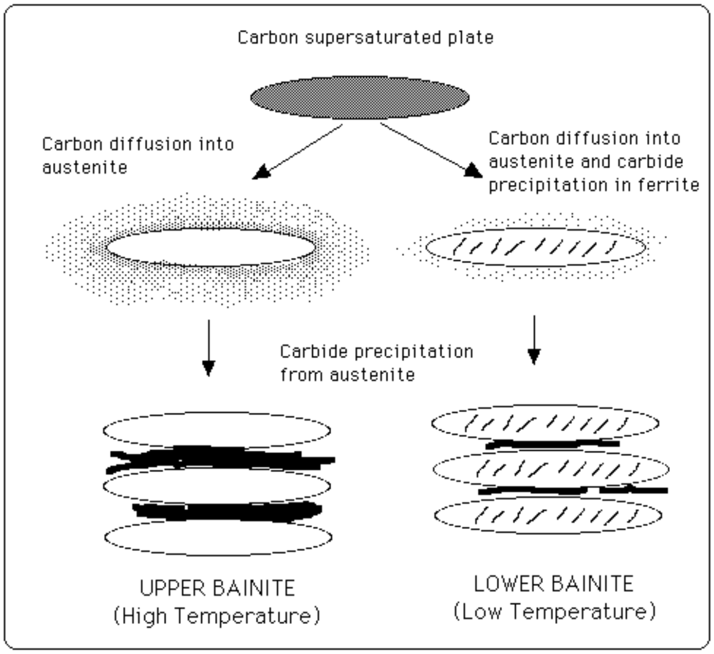

Fig. 1: An illustration of the growth of bainite and the development of upper or lower bainite.

of the carbon to precipitate from supersaturated bainitic ferrite. The remainder partitions into the residual austenite, giving the classical lower bainitic microstructure (Fig. 1).

This theory explains a large class of observations, *some* of which are as follows:

1. There is an invariant–plane strain shape deformation associated with the formation of bainite [8–11]. This deformation has a large shear component [10,11] and given the small diffusion coefficient of iron, implies a coordinated movement of atoms. Such disciplined movements cannot be sustained across grain boundaries of the parent phase, so plates of bainite are confined to the grains in which they grow. This is quite unlike reconstructive transformation products such as allotriomorphic or massive ferrite and pearlite, which are not hindered by austenite grain boundaries.

2. The shape deformation induces plastic accommodation in the adjacent austenite, causing a loss of coherency at the transformation interface and bringing the growth process to a premature halt, *i.e.* before the plate encounters a hard obstacle such as a grain boundary [12]. Subsequent growth then has to occur by the nucleation of new plates, giving rise to the observed sheaf microstructure [2,12]. Notice that there is no mechanism by which a phase that grows by a reconstructive mechanism can be halted in this way before equilibrium is reached.

3. Substitutional elements do not partition even on the finest conceivable scale, as proven by direct atomic resolution images and atomic resolution chemical analysis experiments [4]. These observations are only consistent with a displacive transformation mechanism.

4. In steels where carbide precipitation is prevented, the transformation stops at a point where diffusionless growth becomes thermodynamically impossible. It remains incom-

plete in the sense that the chemical potentials are not uniform at the point where the bainite reaction stops [4].

5. The product grows in the form of thin plates in order to minimise the strain energy due to the shape deformation. Once the reaction has stopped, continued annealing of a mixture of bainitic ferrite plates and residual austenite allows the formation of ferrite at grossly retarded rates by a reconstructive mechanism in which there is no invariant–plane strain (IPS) shape deformation with a large shear component [13].

The theory has also made a number of exciting quantitative predictions which have subsequently been verified experimentally. For example, it predicted that unlike the textbook story, both upper and lower bainite need not form in all steels [7]. It is possible in high–carbon steels to avoid completely the formation of upper bainite so that the pearlite transformation gives way directly to lower bainite as the transformation temperature is reduced. Similarly, in low carbon steels it is possible for the upper bainite reaction to be replaced directly by martensite at lower temperatures, without any intervening lower bainite!

Welds frequently contain intragranularly nucleated upper bainite (the so–called acicular ferrite microstructure). The theory explains why intragranularly nucleated lower bainite is not found in such welds. The low carbon concentration of the vast majority of welding alloys prevents the formation of lower bainite. An experiment in which the carbon concentration was deliberately increased led to the first ever observation of “lower acicular ferrite” [14].

The nucleation part of the theory provides the only explanation for why Widmanstätten ferrite ferrite does not form in all steels, and why some steels only transform to martensite [6].

The response of the bainite transformation to applied elastic stresses can be modelled using standard deformation theory, reinforcing the concept of a displacive transformation mechanism [4,15,16].

It is worth emphasising that the theory, in its quantitative form, has been used in the design of novel steels which are produced commercially. One example is the carbide–free bainitic rail steel with outstanding wear resistance, rolling–contact fatigue strength and low–temperature toughness [17,18]. There are many other developments in progress, which take into account the fact that the reaction stops when diffusionless transformation becomes thermodynamically impossible, three of these can be found in the present proceedings (papers by Kutsov, Jacques and Girault).

## UNRESOLVED ISSUES

There are a number of key issues which are not yet amenable to a full quantitative treatment; of these, the following are probably the most urgent:

- The measured growth rate of individual plates of bainite is far greater than expected from the theory of diffusion–controlled growth [4,19]. It is clear that bainitic ferrite forms with a large supersaturation of carbon, but the possibility of some interstitial diffusion during growth cannot entirely be ruled out. There are a number of theories about this [20,21,22] but none of them are completely convincing for reasons discussed elsewhere [4, page 167].

- There exists kinetic theory capable of estimating the fraction of bainite obtained during the isothermal transformation of austenite in steels where the reaction is not accompanied by the formation of carbides [23]. The model incorporates the mechanism of transformation but the nature of the fitting constants needs to be understood. This entails a better treatment of autocatalytic nucleation.

- The quantitative modelling of the precipitation of carbides during the bainite transformation is a remarkably neglected area of research. This is all the more surprising given that bainite, in the vast majority of steels, contains carbides. Indeed, there is no quantitative theory for the tempering of martensite!
- There are many features of the transformation of plastically deformed austenite to bainite which are not understood. This is important given the fact that there is large scale production of bainitic steels by thermomechanical processing.

It is the intention in this paper to focus on the last two of the topics listed above, since these are probably the most important from the point of view of contemporary technological developments.

## MECHANISM OF CARBIDE FORMATION

There is a great deal of evidence that the carbides associated with these transformations form by displacive mechanism without the partitioning of substitutional solute. The mechanism must obviously involve the diffusion of carbon, but not of substitutional solutes (X) or iron atoms. Considerable experimental data show that the carbide precipitation associated with bainite and martensite does not lead to a partitioning of substitutional solutes [24–26]. The precipitation can occur under conditions where the diffusion rates of iron and substitutional atoms are incredibly small compared with the rate of precipitation (Fig. 2).

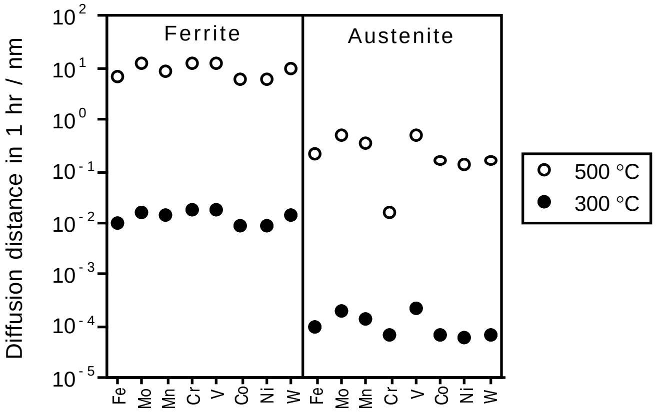

Fig. 2: A $2\sqrt{Dt}$ estimate of the distance diffused in one hour, for iron and some substitutional solutes in iron, as a function of temperature [4]. $D$ is the diffusion coefficient and $t$ the time.

It has in fact been believed for some time that the cementite lattice may be generated by the deformation of the ferrite crystal structure, at a rate controlled by the diffusion of carbon into the appropriate sites. The Fe/X ratio thus remains constant everywhere and subject to that constraint, the carbon achieves equality of chemical potential; the cementite is then said to grow by *paraequilibrium* transformation [27]. The way in which the ferrite lattice could be deformed to produce the right arrangement of iron atoms needed to generate the cementite has been considered by Andrews [28] and Hume–Rothery *et al.* [29], and the subject has been reviewed by Yakel [30]. High–resolution transmission electron microscopy supports the idea that the carbide particles grow by displacive transformation (Sandvik [31], Nakamura and Nagakura [32] and Taylor *et al.* [33,34]).

In a remarkable experiment, Babu *et al.* [35] have shown using the atom–probe technique that the cementite obtained by tempering martensite is forced to inherit the silicon concentration of the martensite. This is in spite of the fact that the equilibrium solubility of silicon in cementite is negligible.

The number of carbide variants which grow in any given plate of martensite decreases when the virgin martensite is tempered under the influence of the stress [36,37]. This response of the microstructure to an externally applied stress is consistent with a displacive mechanism of transformation.

To summarise, it appears that substitutional solute atoms are trapped in the cementite when the latter precipitates during the bainitic or martensitic transformations in steels. That is, the cementite forms by a paraequilibrium transformation mechanism. In silicon containing steels the free energy change associated with the paraequilibrium precipitation of cementite must be much smaller than when the cementite is free of silicon. It is probable that this is what leads to suppression of cementite in high–silicon bainitic or martensitic steels [38]. However, a full theory is far from established and the work is urgent given the technological significance of carbide–free bainitic steels.

A major omission from the array of experimental evidence is that no one has as yet measured the shape deformation due to carbide precipitation. This is because the particles are so incredibly fine, but atomic force microscopy may yet prove possible as an aid to characterising the surface relief.

## KINETICS OF CARBIDE FORMATION

Many of the carbides that form during the bainite transformation are metastable [4]; annealing therefore leads to a series of precipitation reactions which occur together, albeit at different rates. These reactions have been difficult to model given the interactions between the variety of precipitate phases. It is essential to resolve this, both from the point of view of structural steels where silicon is exploited as an alloying element, and for steels used at elevated temperatures where the precipitates control the creep behaviour. A theory is needed to treat the kinetics of simultaneous reactions, and such a theory would naturally be useful in many applications. For example, the tempering of martensite or the ageing of aluminium alloys.

A model for a single transformation begins with the calculation of the nucleation and growth rates using classical theory, but an estimation of the volume fraction requires impingement between particles to be taken into account. This is generally done using the extended volume concept of Johnson, Mehl, Avrami, and Kolmogorov [39] as illustrated in Fig. 3. Suppose that two particles exist at time $t$; a small interval $\delta t$ later, new regions marked $a$, $b$, $c$ & $d$ are formed assuming that they are able to grow unrestricted in extended space whether or not the region into which they grow is already transformed. However, only those components of $a$, $b$, $c$ & $d$ which lie in previously untransformed matrix can contribute to a change in the real volume of the product phase (identified by the subscript ‘1’) so that :

$$dV_1 = (1 - \frac{V_1}{V}) dV_1^e \tag{1}$$

where it is assumed that the microstructure develops randomly. The superscript $e$ refers to extended volume, $V_1$ is the volume of phase 1 and $V$ is the total volume. Multiplying the change in extended volume by the probability of finding untransformed regions has the effect of excluding regions such as $b$, which clearly cannot contribute to the real change in volume of the product. This equation can easily be integrated to obtain the real volume fraction,

$$\frac{V_1}{V} = 1 - \exp\left\{-\frac{V_1^e}{V}\right\} \tag{2}$$

Nucleation and growth rates can readily be substituted into $V_1^e$, leading to the familiar Avrami equation.

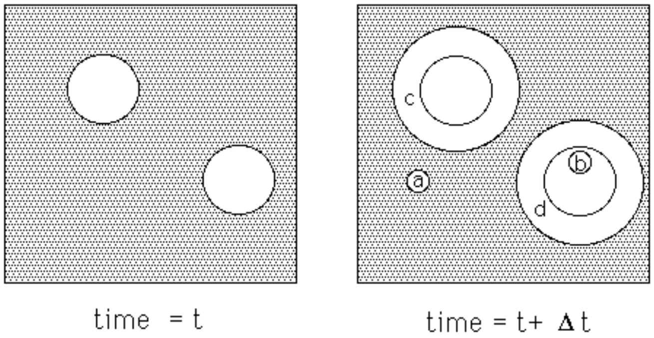

Fig. 3: The concept of extended volume. Two precipitate particles have nucleated and grown to a finite size in the time $t$. New regions $c$ and $d$ are formed as the original particles grow, but $a$ & $b$ are new particles, of which $b$ has formed in a region which is already transformed.

In practice, as stated earlier, there are many cases where several transformations occur together. The different reactions interfere with each other in a way which is seminal to the development of bainitic steel microstructures. The principles involved are first illustrated with an example in which $\beta$ and $\theta$ precipitate at the same time from the parent phase which is designated $\alpha$ [40,41]. For the sake of discussion it is assumed that the nucleation and growth rates do not change with time and that the particles grow isotropically.

The increase in the extended volume due to particles nucleated in a time interval $t = \tau$ to $t = \tau + d\tau$ is, therefore, given by

$$dV_\beta^e = \frac{4}{3}\pi G_\beta^3 (t - \tau)^3 I_\beta(V)\ d\tau \tag{3}$$

$$dV_\theta^e = \frac{4}{3}\pi G_\theta^3 (t - \tau)^3 I_\theta(V)\ d\tau \tag{4}$$

where $G_\beta$, $G_\theta$, $I_\beta$ and $I_\theta$ are the growth and nucleation rates of $\beta$ and $\theta$ respectively, all of which are assumed here to be independent of time. $V$ is the total volume of the system. For each phase, the increase in extended volume will consist of three separate parts. Thus, for $\beta$:

(i) $\beta$ which has formed in untransformed $\alpha$.

(ii) $\beta$ which has formed in regions which are already $\beta$.

(iii) $\beta$ which has formed in regions which are already $\theta$.

Only $\beta$ formed in untransformed $\alpha$ will contribute to the real volume of $\beta$. On average a fraction $\left(1 - \frac{V_\beta + V_\theta}{V}\right)$ of the extended volume will be in previously untransformed material. It follows that the increase in real volume of $\beta$ is given by

$$dV_\beta = \left(1 - \frac{V_\beta + V_\theta}{V}\right) dV_\beta^e \tag{5}$$

and similarly for $\theta$,

$$dV_\theta = \left(1 - \frac{V_\beta + V_\theta}{V}\right) dV_\theta^e \tag{6}$$

Generally $V_\beta$ will be some complicated function of $V_\theta$ and it is not possible to integrate these expressions analytically to find the relationship between the real and extended volumes. Numerical integration is straightforward and offers the opportunity to change the boundary conditions for nucleation and growth as transformation proceeds, to account for the change in the matrix composition during the course of reaction. The method can in principle be applied to any number of simultaneous reactions.

**Complex reactions:** The multiple reactions found in bainitic and martensitic power plant steels have important complications which can all be dealt with in the scheme of simultaneous transformations as presented above. The phases interfere with each other not only by reducing the volume available for transformation, but also by removing solute from the matrix and thereby changing its composition. This change in matrix composition affects the growth and nucleation rates of the phases. The main features of the application of the theory to power plant steels are summarised below; a full description is given in references [40,41].

- The model allows for the simultaneous precipitation of $M_2X$, $M_{23}C_6$, $M_7C_3$, $M_6C$ and Laves phase. $M_3C$ is assumed to nucleate instantaneously with the paraequilibrium composition. Subsequent enrichment of $M_3C$ as it approaches its equilibrium composition is accounted for.
- All the phases, except $M_3C$, form close to their equilibrium composition. The driving forces and compositions of the precipitating phases are calculated using standard thermodynamic methods.
- The interaction between the precipitating phases is accounted for by considering the change in the average solute level in the matrix as each phase forms.
- The model does not require prior knowledge of the precipitation sequence.
- Dissolution of non–equilibrium phases is incorporated as a natural event.

- A single set of fitting parameters for the nucleation equations (site densities and surface energies) has been found which is applicable to a wide range of power plant steels.

The compositions of three power plant alloys used here for illustration purposes, are shown in Table 1. These three alloys, whilst of quite different chemical compositions, show similar precipitation *sequences* but with vastly different rates. For example, at 600 °C the time taken before $M_{23}C_6$ is observed is 1 h in the 10CrMoV steel, 10 h in the 3Cr1.5Mo alloy and in excess of 1000 h in the 2.25Cr1Mo steel [40]. These differences have never before been explained [40,42,43].

| | C | N | Mn | Cr | Mo | Ni | V | Nb |
|---|---|---|---|---|---|---|---|---|
| 2.25Cr1Mo | 0.15 | – | 0.50 | 2.12 | 0.9 | 0.17 | – | – |
| 3Cr1.5Mo | 0.1 | – | 1.0 | 3.0 | 1.5 | 0.1 | 0.1 | – |
| 10CrMoV | 0.11 | 0.056 | 0.50 | 10.22 | 1.42 | 0.55 | 0.20 | 0.50 |

Table 1: Concentration (in weight%) of the major alloying elements in the steels used to demonstrate the model.

## Microstructure Calculations

A plot showing the predicted variation of volume fraction of each precipitate as a function of time at 600 °C is shown in Fig. 4. Consistent with experiments, the precipitation kinetics of $M_{23}C_6$ are predicted to be much slower in the 2.25Cr1Mo steel compared to the 10CrMoV and 3Cr1.5Mo alloys. One contributing factor is that in the 2.25Cr1Mo steel a relatively large volume fraction of $M_2X$ and $M_7C_3$ form prior to $M_{23}C_6$. These deplete the matrix and therefore suppress $M_{23}C_6$ precipitation. The volume fraction of $M_2X$ which forms in the 10CrMoV steel is relatively small, and there remains a considerable excess of solute in the matrix, allowing $M_{23}C_6$ to precipitate rapidly. Similarly, in the 3Cr1.5Mo steel the volume fractions of $M_2X$ and $M_7C_3$ are insufficient to suppress $M_{23}C_6$ precipitation to the same extent as in the 2.25Cr1Mo steel.

$M_{23}C_6$ is frequently observed in the form of coarse particles which are less effective in hindering creep deformation. Delaying its precipitation would have the effect of stabilising the finer dispersions of $M_2X$ and MX to longer times with a possible enhancement of creep strength.

Calculations like these can be used to design microstructures exploiting knowledge built up over decades concerning what is good and bad for creep strength. It is often argued that Laves phase formation is bad for creep resistance – it leads to a reduction in the concentration of solid solution strengthening elements; since the Laves precipitates are few and coarse, they do not themselves contribute significantly to strength. The model presented here can be used to design against Laves phase formation.

We note for the moment, that this is as far as microstructure modelling has progressed. The models are not yet capable of giving size distributions and even if that were to be possible, there are no physical models of creep deformation which have sufficient precision to make use of this information. A great deal of work also needs to be done on realistic methods of taking into account the details of the nucleation process and in tackling soft impingement phenomena in an internally consistent manner.

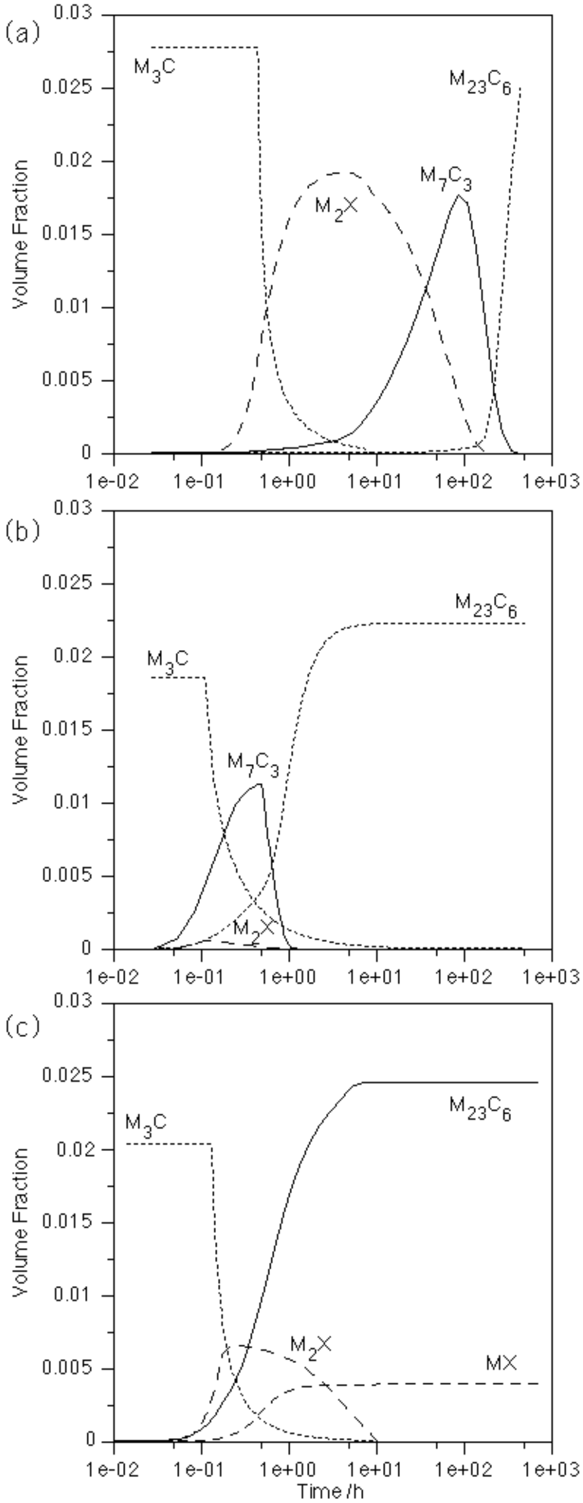

Fig. 4: The predicted evolution of precipitate volume fractions at 600 °C for three power plant materials (a) 2.25Cr1Mo (b) 3Cr1.5Mo and (c) 10CrMoV.

We have emphasised that displacive transformations involve the coordinated movement of atoms, and that such movements cannot be sustained against strong defects such as grain boundaries. Thus, martensite plates, which form by a displacive mechanism, cannot cross grain boundaries. Smaller defects such as isolated dislocations hinder the progress of such transformations, but can often be incorporated into the martensite lattice. However, it is well established [44–49] that the heavy deformation of austenite prior to its transformation hinders the growth of martensite, causing a reduction in the fraction of transformation in spite of an increased rate of heterogeneous nucleation rate due to the greater number density of defects. Another way of visualising this mechanical stabilisation is in terms of the structure of the transformation interface. Displacive transformations are accomplished by the advance of glissile interfaces which can be rendered sessile by the accumulation of dislocation debris. Thus, whereas an appropriate stress can stimulate displacive transformation in the same way that it enables normal deformation [50,51], mechanical stabilisation actually retards the decomposition of the austenite.

Most of the work on mechanical stabilisation effects has been on steels, and has focused on the martensite transformation with very few studies on bainite. Some early experimental data based on hot–rolling experiments [52] can be interpreted to show that bainitic transformation is retarded in deformed austenite, as illustrated in Fig. 5 [4]. More direct evidence comes from the work of Tsuzaki *et al.* [53] who found that although deformed austenite transformed faster, the net volume fraction of bainite that formed decreased when compared with undeformed austenite.

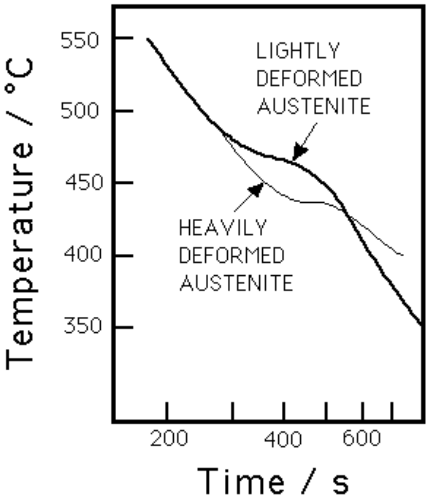

Fig. 5: Plots of temperature versus time, for samples undergoing bainitic transformation during cooling. The deviations from linearity indicate the onset of transformation. The reaction is retarded in the more severely deformed austenite, a manifestation of mechanical stabilisation.

Huang *et al.* [54] showed that deformed austenite transforms to bainite at a higher temperature during continuous cooling and at a faster rate, as long as the cooling occurred sufficiently fast to suppress recovery of the austenite. Similar effects were reported by Smith and Siebert

[55,56].

Maki [57] found that ausforming markedly increases the rate of transformation of upper bainite, with a smaller effect on the lower bainite reaction (the progress of which was eventually retarded). The plates of bainitic ferrite were thinner and contained a larger dislocation density when they grew from deformed austenite. It was concluded that the bainite inherited the defect structure of the austenite. Edwards and Kennon [58] had earlier reported these same observations and in addition, demonstrated nucleation of bainite from slip bands. Freiwillig *et al.* [59] also reported an initial acceleration of transformation to bainite from deformed austenite.

Other studies are more difficult to interpret. In Bhattacharyya and Kehls experiments [60] the bainite was formed from deformed austenite, but under the influence of an applied stress; the latter can complicate interpretation [16]. In microalloyed steels, strain induced precipitation of carbides, carbonitrides or borides can influence the subsequent transformation of austenite [61].

In recent work [62] it has been demonstrated using metallography, that the bainite transformation can be mechanically stabilised in a manner identical to the mechanical stabilisation of martensite in steels (Fig. 6). The mechanism appears to be that the growth of bainite is retarded by the deformation debris in the austenite. Heterogeneous nucleation becomes more frequent as defects are introduced into the austenite, but their growth by a displacive mechanism is stifled as the interface encounters forests of dislocations. Deformed austenite therefore transforms to a smaller quantity of bainite than undeformed austenite, and any bainite that forms is more refined.

Fig. 6: Optical micrographs showing the large effect of mechanical stabilisation in refining the microstructure and in reducing the amount of bainitic transformation. (a) Transformation from undeformed austenite. (b) Transformation from plastically deformed austenite.

The mechanical stabilisation is also evident in quantitative experiments, for example, when the transformation is monitored using dilatometric techniques [63], Fig. 7. There are two puzzling features illustrated, first that transformation from deformed austenite leads to a smaller terminal fraction of bainite. The second feature is that although the transformation rate is at first is accelerated by deformation, it is eventually retarded. If this initial acceleration is explained by increasing the number density of nuclei then it is not possible to reach a smaller terminal fraction given that each nucleus transforms a fixed volume of austenite. On the other hand, if it is assumed that the smaller limiting fraction is due to the reduction in volume transformed per nucleus then it is not possible to explain the initial acceleration. There are other complications described elsewhere, all of which can only be resolved by arguing that the austenite is inhomogeneously deformed [64]. The lightly deformed regions transform more rapidly relative to undeformed austenite because of the increase in the defect density. The nucleation rate is larger in the heavily deformed regions but the overall rate of transformation is reduced because each nucleus then transforms to a smaller volume due to mechanical stabilisation of the interface.

This qualitative theory needs to be developed in much more detail, and has to be backed by direct metallographic observations of the distribution of bainite sub–unit sizes. Such a distribution should be bimodal. The importance of such work cannot be underemphasised given the increasing use of thermomechanical processing of bainitic steels.

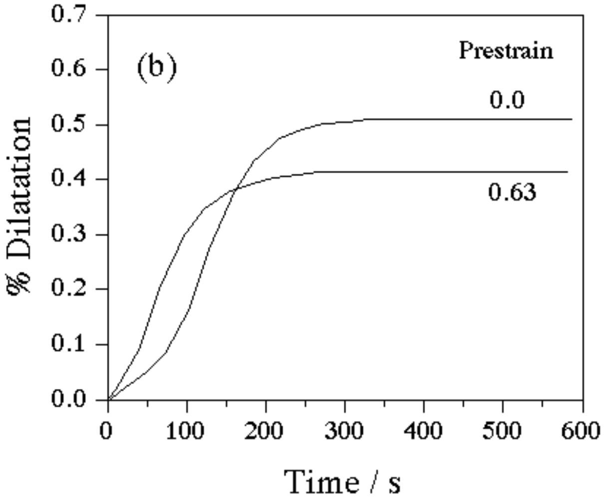

Fig. 7: Change in radial dilatation during isothermal transformation to bainite as a function of time and prestrain (the strain in the austenite prior to transformation); values of the prestrain are indicated next to individual curves.

Mechanical stabilisation has been found to occur for all of the plate–shaped ferritic phases that occur in steels. This includes Widmanstätten ferrite [65], bainite and martensite, all of which cause an invariant–plane strain shape deformation with a large shear component on transformation. Indeed, mechanical stabilisation has been shown to occur in materials as diverse as lithium and brass (see other papers in this conference). On the other hand, reconstructive transformations are without exception accelerated when they occur from the deformed parent phase. This is because there is not only an increase in the number density of nucleation sites in deformed austenite, but the defects are destroyed by the growth of the new phase, akin to what happens in recrystallisation. This is unlike displacive transformations where the defects are inherited by the growing phase. The defects therefore add to the driving force for reconstructive transformation. With these general observations it is possible to define a disarmingly simple criterion to distinguish these two mechanisms of transformation:

> There is no mechanism by which plastic deformation can retard reconstructive transformation. Likewise, only displacive transformations can be mechanically stabilised.

Finally, there are other effects to do with stress and strain affected transformations for which there are only qualitative explanations. One of the most important criterion in steel design is the grain size, in the case of bainite the plate thickness. A recent empirical analysis [66] based on the neural network technique has identified, in descending order of importance, the austenite strength, the driving force for nucleation and the temperature as the variables controlling the thickness of bainite plates (Fig. 8).

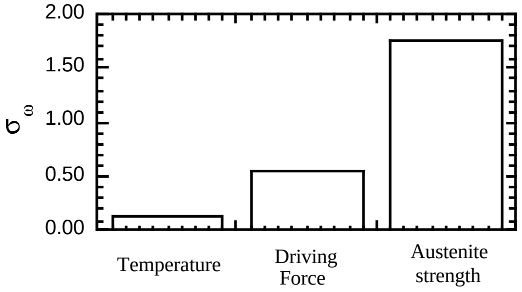

Fig. 8: The model perceived significance of the input variables in influencing the bainite plate thickness. A large value of the parameter $\sigma_w$ implies that the variable concerned is most effective in explaining the variation in the bainite plate thickness.

## CONCLUSIONS

We have seen that the theory for the bainite transformation is at a sufficiently advanced stage to allow its use in the design of novel steels. It is the personal opinion of the author that the next major advances will be in: (a) the understanding of the carbide precipitation reactions that are associated with bainite and (b) the interaction of defects induced by plastic deformation on the kinetics and microstructure of bainite. It was in 1989 that I was asked to present a few unresolved problems in the theory of phase transformations in the context of high–resolution microanalytical techniques [67]. I believe that three of the four problems presented then have now essentially been solved. I therefore look forward to 2009 to assess the value of the work presented here!

## ACKNOWLEDGMENTS

I would like to express my heartfelt thanks to Drs Marcos Sade, Manfred Ahlers and the team from the Centro Atomico Bariloche, for their kindness and care during my stay in Argentina. This alone went a long way towards making ICOMAT '98 a memorable event. As a bonus, the technical content of the meeting was as breathtaking as the local scenery.

## REFERENCES

1. S. Hawkins: A Brief History of Time, Bantam Press, U.S.A., (1988)
2. R. F. Hehemann: Phase Transformations, ASM, Metals Park, Ohio, USA, (1970) 397–432.
3. H. K. D. H. Bhadeshia and J. W. Christian: Metallurgical Transactions A 21A (1990) 767–797.
4. H. K. D. H. Bhadeshia: Bainite in Steels, Institute of Materials, London, (1992) 1–458.
5. R. W. K. Honeycombe and H. K. D. H. Bhadeshia: Steels, Edward Arnold, London, (1995) 115–139.
6. H. K. D. H. Bhadeshia: Acta Metallurgica 29 (1981) 1117–1130.
7. M. Takahashi and H. K. D. H. Bhadeshia: Materials Science and Technology 6 (1990) 592–603.
8. T. Ko and S. A. Cottrell: J. I. S. I. 175 (1952) 307–313.
9. G. R. Srinivasan and C. M. Wayman: Acta Metallurgica 16 (1968) 609–636.
10. B. P. J. Sandvik: Metallurgical Transactions A 13A (1982) 777–800.
11. E. Swallow and H. K. D. H. Bhadeshia: Materials Science and Technology 12 (1996) 121–125.
12. H. K. D. H. Bhadeshia and D. V. Edmonds: Metallurgical Transactions A 10A (1979) 895–907.
13. H. K. D. H. Bhadeshia: International Conference on Solid→Solid Phase Transformations, eds H. I. Aaronson *et al.*, TMS–AIME, Warrendale, PA, U. S. A., (1981) 1041–1048.
14. A. A. B. Sugden and H. K. D. H. Bhadeshia: Metallurgical Transactions A 20A (1989) 1811–1818.
15. H. K. D. H. Bhadeshia, S. A. David, J. M. Vitek and R. W. Reed: Materials Science and Technology 7 (1991) 686–698.
16. A. Matsuzaki, H. K. D. H. Bhadeshia and H. Harada: Acta Metallurgica et Materialia 42 (1994) 1081–1090.
17. J. K. Yates: Science in Parliament 53 (1996) 2–3.
18. H. K. D. H. Bhadeshia: Future Developments of Metals and Ceramics, eds J. A.

Charles, G. W. Greenwood and G. C. Smith, Institute of Materials, London, (1992) 25–75.

19. H. K. D. H. Bhadeshia: Phase Transformations in Ferrous Alloys, eds A. R. Marder and J. I. Goldstein, TMS–AIME, Warrendale, PA, U. S. A., (1984) 335–340.
20. M. Hillert: Metall. Trans. A 6A (1975) 5–19.
21. J. Agren: Acta Metallurgica 37 (1989) 181–189.
22. G. B. Olson, H. K. D. H. Bhadeshia and M. Cohen: Metallurgical Transactions A 21A (1990) 805–809.
23. N. Chester and H. K. D. H. Bhadeshia: Journal de Physique IV, Colloque C5 7 (1997) 41–46.
24. H. K. D. H. Bhadeshia: Materials Science and Technology 5 (1989) 131–137.
25. S. V. Tsivinsky, L. I. Kogan and R. I. Entin: Problems of Metallography and the Physics of Metals, B. Ya Lybubov editor, State Scientific Press, Moscow (Translation published by the Consultants Bureau Inc., New York, 1959) (1955) 185–1991.
26. J. Chance and N. Ridley: Metallurgical Transactions A 21A (1981) 1205–1213.
27. A. Hultgren: Jernkontorets Ann. 135 (1951) 403.
28. K. W. Andrews: Acta Metall. 11 (1963) 939–946.
29. W. Hume–Rothery, G. V. Raynor and A. T. Little: Arch. Eisenhüttenwes. 145 (1942) 143.
30. H. C. Yakel: Int. Met. Rev. 30 (1985) 17–40.
31. P. J. Sandvik: Metall. Trans. A 13 (1982) 789–800.
32. T. Nakamura and S. Nagakura: Int. Conf. on Martensitic Transformations (ICOMAT–86), The Japan Institute of Metals (1986) 1057–1065.
33. K. A. Taylor, G. B. Olson, M. Cohen and J. B. Vander Sande: Metall. Trans. A 20A (1989) 2749–2765.
34. K. A. Taylor, L. Chang, G. B. Olson, G. D. W. Smith, M. Cohen and J. B. Vander Sande: Metall. Trans. A 20A (1989) 2772–2737.
35. S. S. Babu, K. Hono and T. Sakuri: Applied Surface Science 67 (1993) 321–327.
36. A. Matsuzaki, H. K. D. H. Bhadeshia and H. Harada: G. R. Speich symposium, Iron and Steel Society, AIME, Warrendale, PA, U.S.A., ( 1992) 47–52.
37. J. Stewart, R. C. Thomson and H. K. D. H. Bhadeshia: Journal of Materials Science 29 (1994) 6079–6084.
38. M. Lord: Ph.D. Thesis, University of Cambridge (1999)
39. J. W. Christian: Theory of Transformations in Metals and Alloys, Part I, 2nd edition, Pergamon Press, Oxford, (1975)

40. J. Robson and H. K. D. H. Bhadeshia: Materials Science and Technology 13 (1997) 631–639.

41. S. Jones and H. K. D. H. Bhadeshia: Acta Materialia 45 (1997) 2911–2920.

42. J. Robson and H. K. D. H. Bhadeshia: Calphad 20 (1996) 447–460.

43. J. Robson and H. K. D. H. Bhadeshia: Microstructural Stability of Creep Resistant Alloys for High Temperature Plant Applications, eds A. Strang, J. Cawley and G. W. Greenwood, Institute of Materials (1998) 395–404.

44. E. S. Machlin and M. Cohen: Trans. AIME 191 (1951) 746–754.

45 . H.C. Fiedler, B.L. Averbach and M. Cohen: Trans. ASM 47 (1955) 267–290.

46. W.C. Leslie and R.L. Miller: ASM Trans. Quarterly 57 (1964) 972–979.

47. J.R. Strife, M.J. Carr and G.S. Ansell: Metall. Trans. A 8A (1976) 1471–1484.

48. V. Raghavan: Martensite, a tribute to Morris Cohen, ed. G.B. Olson and W.S. Owen, ASM International, Materials Park, OH, U.S.A., (1992) 197–226.

49. K. Tsuzaki, S. Fukasaku, Y. Tomota and T. Maki: Mater. Trans. JIM 32 (1991) 222–228.

50. J.R. Patel and M. Cohen: Acta Metall. 1 (1953) 531–538.

51. J.W. Christian: Metall. Trans. A 13 (1982) 509–538.

52. A.T. Davenport: The Hot Deformation of Austenite , ed. J.B. Ballance, TMS–AIME, New York, U.S.A., (1977) 517–536.

53. K. Tsuzaki, T. Ueda, K. Fujiwara and T. Maki: Proc. 1st Japan International SAMPE Symposium and Exhibition, eds N. Igata *et al.*, Society for advancement of materials and process engineering, Japan, (1989) 799–804.

54. C.Y. Huang, J.R. Yang and S.C. Wang: Mat. Trans. JIM 34 (1993) 658–668.

55. Y.E. Smith and C.A. Siebert: Applications of modern metallographic techniques, ASTM STP 480, American Society for Testing of Materials, (1970) 131–151.

56. Y.E. Smith and C.A. Siebert: Metall. Trans. 2 (1971) 1711–1725.

57. T. Maki: Physical metallurgy of direct–quenched steels, eds K. A. Taylor *et al.*, The Minerals, Metals and Materials Society, Warrendale, U.S.A. (1993) 3–16.

58. R.H. Edwards and N.F. Kennon: Metall. Trans. A 9A (1978) 1801–1809.

59. R. Freiwillig, J. Kudrman and P. Chraska: Metall. Trans. A 1976 (7A) 1091–1097.

60. S. Bhattacharyya and G.L. Kehl: Trans. ASM. 47 (1955) 351–379.

61. H. Tamehiro, M. Murata and R. Habu: HSLA steels: Metallurgy and applications, eds J. Gray *et al.*, ASM International, (1986) 325.

62. P. Shipway and H. K. D. H. Bhadeshia: Materials Science and Metallurgy 11 (1995) 1116–1128.

63. S. B. Singh and H. K. D. H. Bhadeshia: Materials Science and Metallurgy 12 (1996) 610–612.

64. S. B. Singh: Ph.D. Thesis, University of Cambridge, (1998)

65. P. Shipway and H. K. D. H. Bhadeshia: Materials Science and Engineering A 223 (1997) 179–185.

66. S. B. Singh and H. K. D. H. Bhadeshia: Materials Science and Engineering A A245 (1998) 72–79.

67. H. K. D. H. Bhadeshia: Colloque de Physique C8–50 (1989) 395.

# FIGURE CAPTIONS

Figure 1: An illustration of the growth of bainite and the development of upper or lower bainite.

Figure 2: A $2\sqrt{Dt}$ estimate of the distance diffused in one hour, for iron and some substitutional solutes in iron, as a function of temperature [4]. $D$ is the diffusion coefficient and $t$ the time.

Figure 3: The concept of extended volume. Two precipitate particles have nucleated and grown to a finite size in the time $t$. New regions $c$ and $d$ are formed as the original particles grow, but $a$ & $b$ are new particles, of which $b$ has formed in a region which is already transformed.

Figure 4: The predicted evolution of precipitate volume fractions at 600 °C for three power plant materials (a) 2.25Cr1Mo (b) 3Cr1.5Mo and (c) 10CrMoV.

Figure 5: Plots of temperature versus time, for samples undergoing bainitic transformation during cooling. The deviations from linearity indicate the onset of transformation. The reaction is retarded in the more severely deformed austenite, a manifestation of mechanical stabilisation.

Figure 6: Optical micrographs showing the large effect of mechanical stabilisation in refining the microstructure and in reducing the amount of bainitic transformation. (a) Transformation from undeformed austenite. (b) Transformation from plastically deformed austenite.

Figure 7: Change in radial dilatation during isothermal transformation to bainite as a function of time and prestrain (the strain in the austenite prior to transformation); values of the prestrain are indicated next to individual curves.

Figure 8: The model perceived significance of the input variables in influencing the bainite plate thickness. A large value of the parameter $\sigma_w$ implies that the variable concerned is most effective in explaining the variation in the bainite plate thickness.